

Quantum Fisher information from randomized measurements

Aniket Rath,¹ Cyril Branciard,² Anna Minguzzi,¹ and Benoît Vermersch^{1,3,4}

¹Université Grenoble Alpes, CNRS, LPMMC, 38000 Grenoble, France

²Université Grenoble Alpes, CNRS, Grenoble INP, Institut Néel, 38000 Grenoble, France

³Center for Quantum Physics, University of Innsbruck, Innsbruck A-6020, Austria

⁴Institute for Quantum Optics and Quantum Information of the Austrian Academy of Sciences, Innsbruck A-6020, Austria

(Dated: March 6, 2022)

The quantum Fisher information (QFI) is a fundamental quantity of interest in many areas from quantum metrology to quantum information theory. It can in particular be used as a witness to establish the degree of multi-particle entanglement in quantum many-body-systems. In this work, we use polynomials of the density matrix to construct monotonically increasing lower bounds that converge to the QFI. Using randomized measurements we propose a protocol to accurately estimate these lower bounds in state-of-art quantum technological platforms. We perform numerical analysis to obtain the number of measurements required to overcome statistical errors for the lower bound estimates and provide two examples of applications of the method in quantum systems made of coupled qubits and collective spins.

First introduced in quantum metrology to measure the ability for quantum states to perform interferometry beyond the shot-noise limit [1, 2], the quantum Fisher information (QFI) is a fundamental quantity that plays an important role in different fields, including quantum information theory and many-body physics. As quantum states that are metrologically useful are necessarily multipartite entangled [3], the QFI has raised significant interest as a witness of entanglement. In particular, the notion of entanglement ‘depth’—the minimum number of entangled particles in a given state—can be related to the value of the QFI [4]. In many-body physics, the ability for the QFI to reveal the entanglement of mixed states makes it a key quantity in the study of spin models, revealing in particular universal entanglement properties of quantum states crossing a phase transition at finite temperature [5]. This letter presents a protocol to estimate the quantum Fisher information in state-of-art quantum devices via randomized measurements.

The challenge to measure the quantum Fisher information is due to the fact that it is a highly non-linear function of the density matrix. For a given observable A , the QFI of a quantum state ρ can be written in a closed form as

$$F_Q = 2 \text{Tr} \left(\frac{(\rho \otimes \mathbb{1} - \mathbb{1} \otimes \rho)^2}{\rho \otimes \mathbb{1} + \mathbb{1} \otimes \rho} \mathbb{S}(A \otimes A) \right), \quad (1)$$

where \mathbb{S} is the swap operator defined through its action on basis states $|i\rangle$, $|j\rangle$ by $\mathbb{S}(|i\rangle \otimes |j\rangle) = |j\rangle \otimes |i\rangle$. We clarify the form of Eq. (1)—noting in particular that the fraction notation is allowed by the fact that the numerator and denominator commute—and relate it to the more standard expression of the QFI in the Supplemental Material (SM). For pure states $\rho = |\psi\rangle \langle \psi|$, the QFI is proportional to the variance of the operator A , $F_Q = 4(\langle \psi | A^2 | \psi \rangle - \langle \psi | A | \psi \rangle^2)$. The QFI also enters in an inequality certifying multipartite entanglement of the state ρ : in the context of N spins-1/2, if A is a collective

spin operator $A = \frac{1}{2} \sum_{l=1}^N \sigma_\mu^{(l)}$ with $\sigma_\mu^{(l)}$ being the Pauli spin matrix in an arbitrary direction μ that acts on the l^{th} spin, then the condition $F_Q > N$ certifies that a state is entangled and is metrologically useful according to the quantum Cramér-Rao relation [3, 4]. More generally, the QFI can be used to test the k -producibility (a decomposition into a statistical mixture of tensor products of k -particle states) or the m -separability (a decomposition into a statistical mixture of products of at least m factors) of the state ρ [6–8]. In particular, the inequality $F_Q > \Gamma(N, k)$, with $\Gamma(N, k) = \lfloor \frac{N}{k} \rfloor k^2 + (N - \lfloor \frac{N}{k} \rfloor k)^2$, implies that a state is not k -producible, i.e. that it has an entanglement depth of at least $k + 1$. One can show that the QFI is above a certain threshold value by measuring a *lower bound* of it. This includes quantities associated with the expectation value of an observable, such as spin squeezing [3, 9–13], or multiple quantum coherence [14]. Recently, non-linear lower bounds to the QFI, which are not accessible by standard observable measurements, have also been introduced [15–18] and measured [19]. However, the finite distance between these bounds and the QFI typically limits the ability to certify quantum states for metrology, or to detect multipartite entanglement. If the quantum state is in a thermal state, the QFI can also be measured via dynamical susceptibilities [20]. However, the states used in the context of quantum metrology [4], and many-body dynamics [21], are usually out of equilibrium.

Here, we propose a systematic and state-agnostic way to estimate the QFI by measuring a converging series of monotonically increasing approximations F_n , $F_0 \leq F_1 \leq \dots \leq F_Q$, which rapidly tend to F_Q as n increases. Thus, each F_n , being a lower-bound to the QFI, allows one to verify the quantum metrological advantage and/or multipartite entanglement of the quantum state ρ . Moreover, each function F_n , being a *polynomial* function of the density matrix ρ , can be accessed by randomized measurements. Such protocols only re-

quire single qubit random rotations and measurements and have been successfully applied to obtain Rényi entropies [22–26], negativities [27–30], state overlaps [31] (which lead to the sub-QFI, a lower bound on the QFI measured in Ref. [19]), scrambling [32, 33] and topological invariants [34, 35]. Note that conditions on multipartite entanglement can also be expressed in terms of statistical moments of randomized measurements [36–40].

We shall now present our construction of the converging series F_n , and then describe our protocol to access such quantities via randomized measurements both in qubit and collective spin systems, including a detailed study on statistical errors.

Construction of converging lower bounds— We define our polynomial construction of lower bounds F_n for an observable A and a state ρ as

$$F_n = 2 \text{Tr} \left(\sum_{\ell=0}^n (\rho \otimes \mathbb{1} - \mathbb{1} \otimes \rho)^2 (\mathbb{1} \otimes \mathbb{1} - \rho \otimes \mathbb{1} - \mathbb{1} \otimes \rho)^\ell \mathbb{S}(A \otimes A) \right). \quad (2)$$

The construction of the above bounds is detailed in the SM, where it is shown that $\forall n \in \mathbb{N}$, $F_n \leq F_Q$ and $F_n \leq F_{n+1}$ with the inequalities saturating for pure and fully mixed states. For instance, for the first two terms, we obtain

$$F_0 = 4 \text{Tr}(\rho^2 A^2 - \rho A \rho A), \quad (3)$$

$$F_1 = 2F_0 - 4 \text{Tr}(\rho^3 A^2 - \rho^2 A \rho A). \quad (4)$$

Note that the quantity F_0 was shown to be a lower bound of the QFI in Refs. [15, 16], while the sub-QFI of Refs. [18, 19] is a lower bound to F_0 . As shown in the SM, the constructed series F_n converges exponentially with n to F_Q .

Fig. 1(a) illustrates this convergence for different purities of the noisy GHZ state $\rho(p) = (1-p)|\text{GHZ}_N\rangle\langle\text{GHZ}_N| + p\mathbb{1}/2^N$ with $|\text{GHZ}_N\rangle = (|0\rangle^{\otimes N} + |1\rangle^{\otimes N})/\sqrt{2}$, and $A = \frac{1}{2} \sum_{l=1}^N \sigma_z^{(l)}$ (where in order to maximize the QFI obtained for this state, we choose the direction $\mu = z$ for A). GHZ states of up to 20 qubits have been realized in recent quantum platforms [41–43]. This class of states can be used to achieve enhanced sensitivities in quantum metrology [4] as they exhibit non-trivial multipartite entanglement, which cannot be detected using spin-squeezing inequalities [4]. As an important consequence of having a series of monotonically increasing bounds, we can detect multipartite entanglement more and more efficiently as n increases. This is illustrated in Fig. 1(b), where for various values of N and k , we consider the maximal value p^* , such that an entanglement depth of at least $k+1$ can be detected via the inequality $F_n > \Gamma(N, k)$ (which implies $F_Q > \Gamma(N, k)$). The noise tolerance p^* increases as a function of the order n of the lower bounds and is upper bounded by the p^* value corresponding to F_Q .

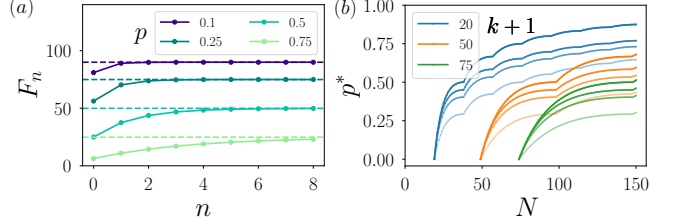


FIG. 1. *Convergence of the lower bounds and entanglement depth certification*— Panel (a) shows the QFI (dashed lines) and its lower bounds F_n as a function of the order n (dots connected by solid lines) for a 10-qubit GHZ state mixed with different white noise strengths p (see legend). The nature of convergence of F_n is commented in the SM. Panel (b) shows for noisy GHZ states, the threshold value of white noise p^* as a function of the number of qubits N for the detection of different entanglement depths of (at least) $k+1$ (see legend) by F_0 , F_1 , F_2 and F_Q (light to dark).

Randomized measurement protocol— Let us now show how the bounds F_n can be accessed from randomized measurements. Such protocols were first shown to give access to the purity $\text{Tr}(\rho^2)$ [23], and then later to any polynomial of the density matrix [25, 28, 29, 44]. What makes our bounds F_n accessible from randomized measurements data is precisely that they are polynomials of ρ (of order $n+2$).

A schematic of the protocol is shown in Fig. 2(a). For concreteness, we first consider a system of N qubits, and develop the corresponding approach for collective spin systems further below. For the randomized measurement protocol, the N -qubit quantum state ρ is prepared in the experiment and we apply local random unitaries u_i sampled from the circular unitary ensemble (CUE) (or a unitary 2-design [45]). We then record as a bit-string $s = s_1, \dots, s_N$ the outcomes of a measurement in a fixed computational basis. This sequence is repeated for M distinct unitaries $u = u_1 \otimes \dots \otimes u_N$, for which classical bit-strings $s^{(r)}$ with $r = 1, \dots, M$ are stored [46].

From this data, we have in principle enough information to reconstruct the density matrix in the limit $M \rightarrow \infty$ [47–49]. To access directly the function F_n , we use the classical shadow formalism [44], and assign to each recorded bit-string $s^{(r)} = s_1^{(r)}, \dots, s_N^{(r)}$ an operator

$$\hat{\rho}^{(r)} = \bigotimes_{i=1}^N \left[3(u_i^{(r)})^\dagger |s_i^{(r)}\rangle\langle s_i^{(r)}| u_i^{(r)} - \mathbb{1}_2 \right]. \quad (5)$$

The operator $\hat{\rho}^{(r)}$ is known as a ‘classical shadow’ in the sense that the average over the unitaries and the bit-string measurement results gives $\mathbb{E}[\hat{\rho}^{(r)}] = \rho$. For different independently sampled shadows labelled r, r' , we obtain similarly that $\hat{\rho}^{(r)}\hat{\rho}^{(r')}$ are unbiased estimations of ρ^2 [44]. This approach that uses the concept of U -statistics [50] generalizes to estimate any power ρ^j , based on using j different shadows $\hat{\rho}^{(r_1)}, \dots, \hat{\rho}^{(r_j)}$. By linear-

ity, this allows one to write the unbiased estimator \hat{F}_n of F_n using combinations of $M \geq n + 2$ different shadows $\rho^{(r)}$. In particular, for $n = 0, 1$, from Eqs. (3)–(4) we obtain the following unbiased estimators for F_0 and F_1 , respectively:

$$\hat{F}_0 = \frac{4}{2!} \binom{M}{2}^{-1} \sum_{r_1 \neq r_2} \text{Tr}(\hat{\rho}^{(r_1)} \hat{\rho}^{(r_2)} A^2 - \hat{\rho}^{(r_1)} A \hat{\rho}^{(r_2)} A), \quad (6)$$

$$\hat{F}_1 = 2\hat{F}_0 - \frac{4}{3!} \binom{M}{3}^{-1} \sum_{r_1 \neq r_2 \neq r_3} \text{Tr}(\hat{\rho}^{(r_1)} \hat{\rho}^{(r_2)} \hat{\rho}^{(r_3)} A^2 - \hat{\rho}^{(r_1)} \hat{\rho}^{(r_2)} A \hat{\rho}^{(r_3)} A). \quad (7)$$

We stress that, although the experimental setting required for randomized measurements are the same as for quantum state tomography, there are some distinct differences. Firstly, the number of measurements required to overcome shot noise errors can be of the order of 8^N for quantum state tomography [51, 52], while for randomized measurements this number scales as 2^{aN} with $a \sim 1$ [23, 31, 32]. In addition, randomized measurement protocols can be optimized using importance sampling, leading to drastic reductions of the required number of measurements [53–56]. Secondly in tomography the classical post-processing of the measurement data is expensive, as it is based on storing and manipulating exponentially large matrices. In contrast, the use of classical shadows in randomized measurements, which have a tensor product structure, c.f. Eq. (5), lead to estimation algorithms that are both cheap in postprocessing runtime and memory usage [28, 44].

Statistical errors — Statistical errors associated with the estimation of F_n arise due to the application of a finite number of random unitary transformations M . In particular, as n increases, while the bound F_n becomes tighter the degree of the polynomial in ρ in the estimator \hat{F}_n , evaluated with M different shadows, increases. This suggests that, in order to reach a fixed level of accuracy, one needs more measurements to estimate F_{n+1} when compared to F_n , as seen in other protocols [28, 44].

In order to quantify statistical errors, we first analytically bound the probabilities to obtain estimations in a given confidence interval [28, 44]. As shown in the SM, this analysis shows that in the large- M limit, the variance in estimating the first term F_0 of our series is (at most) proportional to $2^N \text{Tr}[(\rho A^2)^2]/M$, which indicates a similar dependence on the system size N and the state ρ with respect to the measurement of the purity [44].

To complement our analytical study, we now numerically study the error scalings for F_0 and F_1 by simulating the experimental protocol as a function of the number of measurements M for different system sizes N . The average statistical error \mathcal{E} is computed by averaging over 50 simulated experimental runs the relative error $\hat{\mathcal{E}} = |\hat{F}_n - F_n|/F_n$ of the estimated bound \hat{F}_n . As

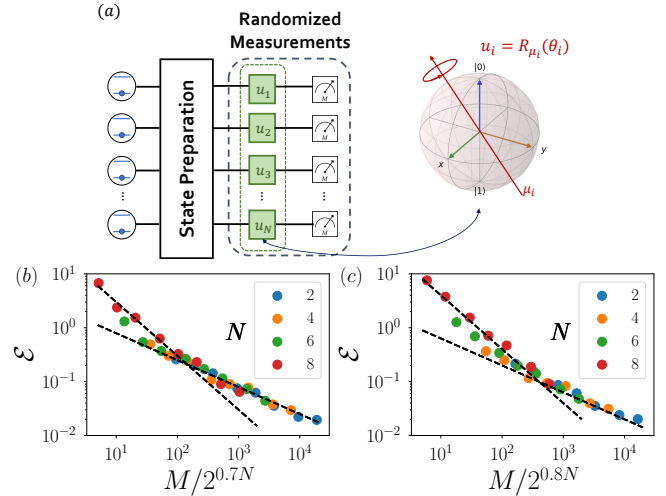


FIG. 2. *Protocol and statistical error scaling* — Panel (a) illustrates the randomized measurement protocol needed to estimate the lower bounds of the QFI. Local random unitaries are applied followed by measurements performed in a fixed computational basis. Panels (b) and (c) show the error scaling for F_0 and F_1 respectively by considering a GHZ state mixed with a depolarisation noise of strength $p = 0.25$, and for various values of N (see legends). The dashed black lines highlight the different error scalings $\propto 1/M$ and $\propto 1/\sqrt{M}$.

above we consider the N -qubit noisy GHZ state with $A = \frac{1}{2} \sum_{l=1}^N \sigma_z^{(l)}$. Fig. 2(b,c) shows the scaling of the average statistical error in estimating F_0 and F_1 , as a function of rescaled number of measurements $M/2^{aN}$ with a being adjusted by collapsing the data obtained for different N onto a single curve. The figures show that the required number of measurements to obtain an error accuracy of 0.1 scales overall as $\sim 2^{0.7N}$ and $\sim 2^{0.8N}$ for F_0 and F_1 respectively. In particular, for large M we observe a $1/\sqrt{M}$ scaling, which is the standard error decay obtained by performing an empirical Monte-carlo average. In the regime of smaller M , the statistical error being high, decays much faster as $1/M$. These two error regimes are also apparent in the expression of the variance (SM). Second, as expected and seen above from the scaling exponents of F_0 and F_1 , we observe that the measurement of F_1 requires slightly more measurements compared to F_0 (see also SM for non-rescaled data). Note that similar error scalings, and the transition from $1/\sqrt{M}$ to $1/M$ behaviors have been observed for other types of cubic order terms related to entanglement negativities [27, 28].

Systematic errors — Present NISQ devices are very often vulnerable to errors due to noise [57]. A typical example of such error could be associated to depolarization or readout errors acting during the measurement phase of our protocol. However, the estimations of the quantities provided by randomized measurements have been shown to be robust in the presence of such noise [26, 31, 58–

[61]. In particular, for a global depolarizing noise, we can assume that the measured bit-strings are sampled from an effective state $\tilde{\rho} = u[(1 - \tilde{p})\rho + \tilde{p}\mathbb{1}/2^N]u^\dagger$. Here, \tilde{p} is the amount of noise occurring during the measurement protocol (not to be confused with the noise strength p describing the state under study). The shadows $\hat{\rho}^{(r)}$ will lead to systematic errors in estimating F_n , as the state $\tilde{\rho}$ is more noisy than the original one ρ . However, noting that $\mathbb{E}[\hat{\rho}^{(r)}] = (1 - \tilde{p})\rho + \tilde{p}\mathbb{1}/2^N$, we can define corrected shadows $\hat{\rho}_c^{(r)} = (\hat{\rho}^{(r)} - \tilde{p}\mathbb{1}/2^N)/(1 - \tilde{p})$ that reconstructs the original state ρ in expectation i.e. $\mathbb{E}[\hat{\rho}_c^{(r)}] = \rho$. This provides estimations of F_n that are immune to the measurement noise \tilde{p} . Note that in order to be able to correct these systematic errors occurring in the course of our protocol, we need a good knowledge on the type and amount of noise (e.g. here, depolarizing noise with strength \tilde{p}).

Protocol for collective spin systems— We now extend our approach to an ensemble of N particles described by a collective spin $S = \frac{N}{2}$. These systems implemented with ultracold atoms or trapped ions, are relevant to quantum metrology [9–12, 20] as they can feature large-scale multipartite entanglement [13]. Remarkably, our protocol provides access to the series F_n in these systems with relatively low numbers of measurements M .

Consider for concreteness a set of N ultracold bosons in a double-well potential, as illustrated in Fig. 3(a). It is convenient to write the state of the system in terms of $N+1$ Fock states $|n_1, n_2\rangle$ or $|n_1 - n_2\rangle$ with $n_1 \in 0, \dots, N$, the number of atoms in the left well and $n_2 = N - n_1$ atoms in the right well. The Bose-Hubbard Hamiltonian H_t describing this system reads

$$H_t = \frac{\mathcal{J}}{2}(\hat{a}_{L,R}^\dagger \hat{a}_{L,R} + \text{h.c.}) + \frac{U_{\text{int}}}{2} \sum_{\ell=L,R} \hat{n}_\ell(\hat{n}_\ell - 1) + \Delta_t(\hat{n}_L - \hat{n}_R), \quad (8)$$

where, $\hat{n}_{L,R} = \hat{a}_{L,R}^\dagger \hat{a}_{L,R}$ are the number operators given in terms of creation $\hat{a}_{L,R}^\dagger$ and annihilation $\hat{a}_{L,R}$ operators, \mathcal{J} is the tunneling matrix element, U_{int} is the on-site interaction energy, and Δ_t is a random energy offset, c.f. Fig. 3(a). It can be equivalently written using spin $S = \frac{N}{2}$ operators [62–64]. The random unitaries U can be experimentally generated as $U = e^{-iH_\eta T} \dots e^{-iH_1 T}$ by choosing different random energy difference Δ_η in H_η for some time interval T . The convergence of such unitaries U to unitary 2-designs (which are required in order to build classical shadows) as a function of the depth η has been studied in [23, 58, 65–67]. Note that these unitaries U , considered here for the purpose of randomized measurements, can also be used to generate metrologically useful quantum states [68].

Compared to the situation of N qubits presented above, the protocol to measure the series F_n in this system differs only in applying global random unitaries U instead of local random unitaries u . We first prepare a state ρ of interest in this system, then generate ran-

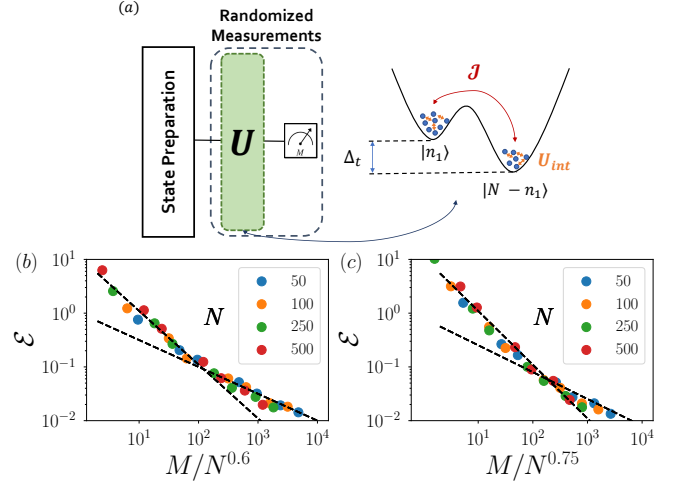


FIG. 3. *Protocol and error scalings for collective spin models*— Panel (a) illustrates the two-site collective spin model followed by the randomized measurement protocol implementing global random unitaries. The lower panels show the statistical error scalings of (b) F_0 and (c) F_1 for a N00N state of bosonic ensembles mixed with depolarisation noise of strength $p = 0.25$ as a function of rescaled axis M/N^a , and for various values of N (see legends).

dom unitaries U followed by measurements of the populations (n_1, n_2) in each well. Repeating this procedure for M unitary matrices $U^{(r)}$, we collect measurement results $s^{(r)} = n_1^{(r)} - n_2^{(r)}$ with $r = 1, \dots, M$. A classical shadow $\hat{\rho}^{(r)}$ of ρ [34, 44, 47] is then constructed from each measurement outcome $s^{(r)}$ and the applied unitary $U^{(r)}$ as

$$\hat{\rho}^{(r)} = \left[(N+2) (U^{(r)})^\dagger |s^{(r)}\rangle \langle s^{(r)}| U^{(r)} - \mathbb{1}_{N+1} \right]. \quad (9)$$

Here, the classical shadow is a matrix of dimension $(N+1) \times (N+1)$. From this, we build our series of estimators \hat{F}_n from the measurement data in the same way as shown earlier for the N -qubit systems.

We investigate the statistical error scalings of our protocol to estimate the lower bounds F_0 and F_1 by computing the average relative error \mathcal{E} . We consider the N00N state given by $|N00N\rangle = \frac{1}{\sqrt{2}}(|N,0\rangle + |0,N\rangle)$ [4]. Such states provide optimal metrological sensitivities and are genuinely multipartite entangled, i.e. they have an entanglement depth of N [4]. The collective spin observable to estimate the lower bound is taken to be the population difference between the two wells and is defined as $A = \hat{n}_1 - \hat{n}_2$. We numerically analyze the scaling of statistical errors of our protocol in these systems by directly generating global random unitaries from the CUE. For simplicity, we study a state $\rho(p) = (1 - p)|N00N\rangle \langle N00N| + p\mathbb{1}/(N+1)$ subject to depolarisation noise of strength $p = 0.25$. Various other noise models have been studied for macroscopic superposition states in [69–72]. Fig. 3(b,c) shows that

the required number of measurements for these states no longer scale exponentially but sub-polynomially in the number of atoms N for F_0 and F_1 . This is attributed to the fact that the Hilbert space dimension scales linearly in N (in contrast, it scales exponentially with N for the qubit protocol). The required number of measurements for obtaining an error of 0.1 is found to scale as N^{a_0} and N^{a_1} with $a_0 \sim 0.6$ and $a_1 \sim 0.75$ for F_0 and F_1 , respectively.

Conclusion and outlook — We have shown how to access the QFI via a converging series of lower bounds. This provides a method for asserting and verifying states capable of providing enhanced metrological sensitivities, as well as for the quantum simulation of many-body systems including non-equilibrium ones. Importantly, via the randomized measurement framework, we can make predictions on the required number of measurements to detect entanglement with a certain confidence interval. As a future direction, it would be interesting to compare the entanglement detection ‘power’ of different protocols based on randomized measurements. This includes in particular approaches based on the positive partial transpose condition [19, 28, 29], which can be applied in the multipartite case [73], and on statistical correlations of Pauli measurements [36–40].

We thank A. Elben and R. Kueng for fruitful discussions, and comments on the manuscript. BV thanks P. Zoller for inspiring discussions and previous collaborations on randomized measurements. AR is supported by Laboratoire d’excellence LANEF in Grenoble (ANR-10-LABX-51-01) and from the Grenoble Nanoscience Foundation. BV acknowledges funding from the Austrian Science Fundation (FWF, P 32597 N). BV and AM acknowledge funding from the French National Research Agency (ANR-20-CE47-0005, JCJC project QRand). For our numerical simulations we used the quantum toolbox QuTiP [74].

[1] S. L. Braunstein and C. M. Caves, *Phys. Rev. Lett.* **72**, 3439 (1994).

[2] S. L. Braunstein, C. M. Caves, and G. J. Milburn, *Annals of Physics* **247**, 135 (1996).

[3] L. Pezzé and A. Smerzi, *Phys. Rev. Lett.* **102**, 100401 (2009).

[4] L. Pezzé, A. Smerzi, M. K. Oberthaler, R. Schmied, and P. Treutlein, *Reviews of Modern Physics* **90**, 35005 (2018).

[5] P. Zanardi, M. G. A. Paris, and L. Campos Venuti, *Phys. Rev. A* **78**, 42105 (2008).

[6] G. Tóth, *Phys. Rev. A* **85**, 22322 (2012).

[7] P. Hyllus, W. Laskowski, R. Krischek, C. Schwemmer, W. Wieczorek, H. Weinfurter, L. Pezzé, and A. Smerzi, *Phys. Rev. A* **85**, 22321 (2012).

[8] Z. Ren, W. Li, A. Smerzi, and M. Gessner, *Phys. Rev. Lett.* **126**, 80502 (2021).

[9] T. Monz, P. Schindler, J. T. Barreiro, M. Chwalla, D. Nigg, W. A. Coish, M. Harlander, W. Hänsel, M. Hennrich, and R. Blatt, *Phys. Rev. Lett.* **106**, 130506 (2011).

[10] H. Strobel, W. Muessel, D. Linnemann, T. Zibold, D. B. Hume, L. Pezzé, A. Smerzi, and M. K. Oberthaler, *Science* **345**, 424 (2014).

[11] G. Barontini, L. Hohmann, F. Haas, J. Estève, and J. Reichel, *Science* **349**, 1317 (2015).

[12] J. G. Bohnet, B. C. Sawyer, J. W. Britton, M. L. Wall, A. M. Rey, M. Foss-Feig, and J. J. Bollinger, *Science* **352**, 1297 (2016).

[13] R. Schmied, J. D. Bancal, B. Allard, M. Fadel, V. Scarani, P. Treutlein, and N. Sangouard, *Science* **352**, 441 (2016).

[14] M. Gärttner, P. Hauke, and A. M. Rey, *Phys. Rev. Lett.* **120**, 040402 (2018).

[15] C. Zhang, B. Yadin, Z.-B. Hou, H. Cao, B.-H. Liu, Y.-F. Huang, R. Maity, V. Vedral, C.-F. Li, G.-C. Guo, and D. Girolami, *Phys. Rev. A* **96**, 042327 (2017).

[16] D. Girolami and B. Yadin, *Entropy* **19**, 124 (2017).

[17] J. L. Beckey, M. Cerezo, A. Sone, and P. J. Coles, *arXiv:2010.10488*.

[18] M. Cerezo, A. Sone, J. L. Beckey, and P. J. Coles, *Quantum Science and Technology* (2021).

[19] M. Yu, D. Li, J. Wang, Y. Chu, P. Yang, M. Gong, N. Goldman, and J. Cai, (2021), *arXiv:2104.00519*.

[20] M. Gärttner, J. G. Bohnet, A. Safavi-Naini, M. L. Wall, J. J. Bollinger, and A. M. Rey, *Nature Physics* **13**, 781 (2017).

[21] R. J. Lewis-Swan, A. Safavi-Naini, A. M. Kaufman, and A. M. Rey, *Nature Reviews Physics* **1**, 627 (2019).

[22] S. J. van Enk and C. W. J. Beenakker, *Phys. Rev. Lett.* **108**, 110503 (2012).

[23] A. Elben, B. Vermersch, M. Dalmonte, J. I. Cirac, and P. Zoller, *Phys. Rev. Lett.* **120**, 50406 (2018).

[24] T. Brydges, A. Elben, P. Jurcevic, B. Vermersch, C. Maier, B. P. Lanyon, P. Zoller, R. Blatt, and C. F. Roos, *Science* **364**, 260 (2019).

[25] V. Vitale, A. Elben, R. Kueng, A. Neven, J. Carrasco, B. Kraus, P. Zoller, P. Calabrese, B. Vermersch, and M. Dalmonte, *arXiv:2101.07814*.

[26] K. J. Satzinger, Y. Liu, A. Smith, C. Knapp, M. Newman, C. Jones, Z. Chen, C. Quintana, X. Mi, A. Dunsworth, C. Gidney, I. Aleiner, F. Arute, K. Arya, J. Atalaya, R. Babbush, J. C. Bardin, J. Basso, A. Bengtsson, A. Bilmes, M. Broughton, B. B. Buckley, D. A. Buell, B. Burkett, B. Chiaro, R. Collins, W. Courtney, S. Demura, A. R. Derk, D. Eppens, C. Erickson, E. Farhi, L. Foaro, A. G. Fowler, B. Foxen, M. Giustina, A. Greene, J. A. Gross, M. P. Harrigan, J. Hilton, S. Hong, T. Huang, W. J. Huggins, L. B. Ioffe, S. V. Isakov, E. Jeffrey, Z. Jiang, K. Kechedzhi, T. Khattar, S. Kim, P. V. Klimov, A. N. Korotkov, F. Kostritsa, D. Landhuis, A. Locharla, E. Lucero, O. Martin, J. R. McClean, M. McEwen, K. C. Miao, M. Mohseni, W. Mruczkiewicz, J. Mutus, O. Naaman, M. Neeley, C. Neill, M. Y. Niu, T. E. O. Brien, A. Opremcak, B. Pat, A. Petukhov, N. C. Rubin, D. Sank, V. Shvarts, D. Strain, M. Szalay, T. C. White, Z. Yao, P. Yeh, J. Yoo, A. Zalcman, H. Neven, S. Boixo, A. Megrant, Y. Chen, J. Kelly, V. Smelyanskiy, A. Kitaev, M. Knap, F. Pollmann, and P. Roushan, *arXiv:2104.01180*.

[27] Y. Zhou, P. Zeng, and Z. Liu, *Phys. Rev. Lett.* **125**,

200502 (2020).

[28] A. Elben, R. Kueng, H.-Y. R. Huang, R. van Bijnen, C. Kokail, M. Dalmonte, P. Calabrese, B. Kraus, J. Preskill, P. Zoller, and B. Vermersch, *Phys. Rev. Lett.* **125**, 200501 (2020).

[29] A. Neven, J. Carrasco, V. Vitale, C. Kokail, A. Elben, M. Dalmonte, P. Calabrese, P. Zoller, B. Vermersch, R. Kueng, and B. Kraus, [arXiv:2103.07443](https://arxiv.org/abs/2103.07443).

[30] X.-d. Yu, S. Imai, and O. Gühne, [arXiv:2103.06897](https://arxiv.org/abs/2103.06897).

[31] A. Elben, B. Vermersch, R. Van Bijnen, C. Kokail, T. Brydges, C. Maier, M. K. Joshi, R. Blatt, C. F. Roos, and P. Zoller, *Phys. Rev. Lett.* **124**, 10504 (2020).

[32] B. Vermersch, A. Elben, L. M. Sieberer, N. Y. Yao, and P. Zoller, *Phys. Rev. X* **9**, 21061 (2019).

[33] M. K. Joshi, A. Elben, B. Vermersch, T. Brydges, C. Maier, P. Zoller, R. Blatt, and C. F. Roos, *Phys. Rev. Lett.* **124**, 240505 (2020).

[34] A. Elben, J. Yu, G. Zhu, M. Hafezi, F. Pollmann, P. Zoller, and B. Vermersch, *Science Advances* **6**, eaaz3666 (2020).

[35] Z.-P. Cian, H. Dehghani, A. Elben, B. Vermersch, G. Zhu, M. Barkeshli, P. Zoller, and M. Hafezi, *Phys. Rev. Lett.* **126**, 050501 (2021).

[36] L. Knips, J. Dziewior, W. Kłobus, W. Laskowski, T. Paterek, P. J. Shadbolt, H. Weinfurter, and J. D. A. Meinecke, *npj Quantum Information* **6**, 51 (2020).

[37] A. Ketterer, N. Wyderka, and O. Gühne, *Phys. Rev. Lett.* **122**, 120505 (2019).

[38] A. Ketterer, N. Wyderka, and O. Gühne, *Quantum* **4**, 325 (2020).

[39] A. Ketterer, S. Imai, N. Wyderka, and O. Gühne, [arXiv:2012.12176](https://arxiv.org/abs/2012.12176).

[40] S. Imai, N. Wyderka, A. Ketterer, and O. Gühne, *Phys. Rev. Lett.* **126**, 150501 (2021).

[41] K. X. Wei, I. Lauer, S. Srinivasan, N. Sundaresan, D. T. McClure, D. Toyli, D. C. McKay, J. M. Gambetta, and S. Sheldon, *Phys. Rev. A* **101**, 032343 (2020).

[42] C. Song, K. Xu, H. Li, Y.-R. Zhang, X. Zhang, W. Liu, Q. Guo, Z. Wang, W. Ren, J. Hao, H. Feng, H. Fan, D. Zheng, D.-W. Wang, H. Wang, and S.-Y. Zhu, *Science* **365**, 574 (2019).

[43] A. Omran, H. Levine, A. Keesling, G. Semeghini, T. T. Wang, S. Ebadi, H. Bernien, A. S. Zibrov, H. Pichler, S. Choi, J. Cui, M. Rossignolo, P. Rembold, S. Montangero, T. Calarco, M. Endres, M. Greiner, V. Vuletić, and M. D. Lukin, *Science* **365**, 570 (2019).

[44] H.-Y. Huang, R. Kueng, and J. Preskill, *Nature Physics* **16**, 1050 (2020).

[45] D. Gross, K. Audenaert, and J. Eisert, *Journal of Mathematical Physics* **48**, 52104 (2007).

[46] Note that, to simplify the experimental procedure, it is also possible to write estimators from randomized measurements based on collecting several bit-strings for each random unitary [28].

[47] M. Ohliger, V. Nesme, and J. Eisert, *New Journal of Physics* **15**, 015024 (2013).

[48] A. Elben, B. Vermersch, C. F. Roos, and P. Zoller, *Phys. Rev. A* **99**, 052323 (2019).

[49] M. Gută, J. Kahn, R. Kueng, and J. A. Tropp, *Journal of Physics A: Mathematical and Theoretical* **53**, 204001 (2020).

[50] W. Hoeffding, in *Breakthroughs in Statistics* (Springer, 1992) pp. 308–334.

[51] D. Gross, Y.-K. Liu, S. T. Flammia, S. Becker, and J. Eisert, *Phys. Rev. Lett.* **105**, 150401 (2010).

[52] J. Haah, A. W. Harrow, Z. Ji, X. Wu, and N. Yu, *IEEE Transactions on Information Theory* **63**, 5628 (2017).

[53] C. Hadfield, S. Bravyi, R. Raymond, and A. Mezzacapo, [arXiv:2006.15788](https://arxiv.org/abs/2006.15788).

[54] A. Rath, R. van Bijnen, A. Elben, P. Zoller, and B. Vermersch, [arXiv:2102.13524](https://arxiv.org/abs/2102.13524).

[55] H.-Y. Huang, R. Kueng, and J. Preskill, [arXiv:2103.07510](https://arxiv.org/abs/2103.07510).

[56] S. Hillmich, C. Hadfield, R. Raymond, A. Mezzacapo, and R. Wille, [arXiv:2105.06932](https://arxiv.org/abs/2105.06932).

[57] J. Preskill, *Quantum* **2**, 79 (2018).

[58] B. Vermersch, A. Elben, M. Dalmonte, J. I. Cirac, and P. Zoller, *Phys. Rev. A* **97**, 23604 (2018), 1801.00999.

[59] S. Chen, W. Yu, P. Zeng, and S. T. Flammia, [arXiv:2011.09636](https://arxiv.org/abs/2011.09636).

[60] D. E. Koh and S. Grewal, [arXiv:2011.11580](https://arxiv.org/abs/2011.11580).

[61] J. Vovrosh, K. E. Khosla, S. Greenaway, C. Self, M. S. Kim, and J. Knolle, [arXiv:2101.01690](https://arxiv.org/abs/2101.01690).

[62] F. T. Arecchi, E. Courtens, R. Gilmore, and H. Thomas, *Phys. Rev. A* **6**, 2211 (1972).

[63] G. J. Milburn, J. Corney, E. M. Wright, and D. F. Walls, *Phys. Rev. A* **55**, 4318 (1997).

[64] G. Ferrini, A. Minguzzi, and F. W. J. Hekking, *Phys. Rev. A* **78**, 023606 (2008).

[65] C. Dankert, R. Cleve, J. Emerson, and E. Livine, *Phys. Rev. A* **80**, 012304 (2009).

[66] L. Banchi, D. Burgarth, and M. J. Kastoryano, *Phys. Rev. X* **7**, 041015 (2017).

[67] L. M. Sieberer, T. Olsacher, A. Elben, M. Heyl, P. Hauke, F. Haake, and P. Zoller, *npj Quantum Information* **5**, 78 (2019).

[68] M. Oszmaniec, R. Augusiak, C. Gogolin, J. Kolodyński, A. Acín, and M. Lewenstein, *Phys. Rev. X* **6**, 041044 (2016).

[69] Y. P. Huang and M. G. Moore, *Phys. Rev. A* **73**, 023606 (2006).

[70] G. Ferrini, D. Spehner, A. Minguzzi, and F. W. J. Hekking, *Phys. Rev. A* **82**, 033621 (2010).

[71] K. Pawłowski, D. Spehner, A. Minguzzi, and G. Ferrini, *Phys. Rev. A* **88**, 013606 (2013).

[72] K. Pawłowski, M. Fadel, P. Treutlein, Y. Castin, and A. Sinatra, *Phys. Rev. A* **95**, 063609 (2017).

[73] B. Jungnitsch, T. Moroder, and O. Gühne, *Phys. Rev. Lett.* **106**, 190502 (2011).

[74] J. Johansson, P. Nation, and F. Nori, *Computer Physics Communications* **184**, 1234 (2013).

SUPPLEMENTAL MATERIAL

The Supplemental Material below provides more detailed discussions on some ideas introduced in the main text. In Appendix A, we detail the proof of our converging polynomial series of lower bounds F_n , followed by the demonstration in Appendix B that these bounds converge exponentially to F_Q as $n \rightarrow \infty$. Next, we go on to elaborate in Appendix C the construction of unbiased estimators \hat{F}_n of F_n from randomized measurements, and then provide in Appendix D the required number of measurements M to estimate F_0 in a given confidence interval with an accuracy ϵ , and with a confidence level δ . Finally in Appendix E, we complement with some additional numerical simulations of our protocol, and the analysis of the scalings of the average statistical errors \mathcal{E} for F_0 and F_1 .

Appendix A: Proof of our lower bounds F_n

In this section we prove that the quantities F_n defined in Eq. (2) of the main text are indeed lower bounds on the quantum Fisher information.

Let us start by clarifying the form of the QFI in Eq. (1). First note that the denominator in the fraction may not be invertible; in that case the fraction denotes a multiplication by the Moore-Penrose pseudoinverse of the denominator; note also that this (pseudo)inverse commutes with the numerator, so that the fraction notation is indeed nonambiguous.

Consider the spectral decomposition of ρ in the form $\rho = \sum_i \lambda_i |i\rangle\langle i|$, with $\lambda_i \geq 0$, $\sum_i \lambda_i = 1$ (all the systems and states we consider are finite-dimensional). Noting that the numerator in the fraction of Eq. (1) is $(\rho \otimes \mathbb{1} - \mathbb{1} \otimes \rho)^2 = (\sum_{i,j} (\lambda_i |i\rangle\langle i| \otimes |j\rangle\langle j| - \lambda_j |i\rangle\langle i| \otimes |j\rangle\langle j|))^2 = \sum_{i,j} (\lambda_i - \lambda_j)^2 |i, j\rangle\langle i, j|$ and that the (pseudo)inverse of the denominator is $(\rho \otimes \mathbb{1} + \mathbb{1} \otimes \rho)^{-1} = (\sum_{i,j} (\lambda_i |i\rangle\langle i| \otimes |j\rangle\langle j| + \lambda_j |i\rangle\langle i| \otimes |j\rangle\langle j|))^{-1} = \sum_{i,j: \lambda_i + \lambda_j > 0} (\lambda_i + \lambda_j)^{-1} |i, j\rangle\langle i, j|$, we find that Eq. (1) can be more explicitly written as

$$F_Q = 2 \sum_{\substack{i,j: \\ \lambda_i + \lambda_j > 0}} \frac{(\lambda_i - \lambda_j)^2}{\lambda_i + \lambda_j} \text{Tr}(|i, j\rangle\langle i, j| \mathbb{S}(A \otimes A)) = 2 \sum_{\substack{i,j: \\ \lambda_i + \lambda_j > 0}} \frac{(\lambda_i - \lambda_j)^2}{\lambda_i + \lambda_j} |\langle i | A | j \rangle|^2, \quad (10)$$

which is indeed the more common closed form for the QFI that one finds in the literature [1, 2].

In order to construct lower bounds on the QFI that can suitably be accessed through randomised measurements, the idea is to bound each factor $\frac{(\lambda_i - \lambda_j)^2}{\lambda_i + \lambda_j}$ by a polynomial function of the eigenvalues λ_i . This can be done by expanding the fraction in a Taylor series (noting that $0 < \lambda_i + \lambda_j \leq 1$), and truncating the series as follows:

$$\frac{1}{\lambda_i + \lambda_j} = \sum_{\ell=0}^{\infty} (1 - \lambda_i - \lambda_j)^\ell \geq \sum_{\ell=0}^n (1 - \lambda_i - \lambda_j)^\ell \quad (11)$$

for any $n \in \mathbb{N}$. Thus expressing Eq. (10) in terms of this expansion gives

$$\begin{aligned} F_Q &= 2 \sum_{i,j} \sum_{\ell=0}^{\infty} (\lambda_i - \lambda_j)^2 (1 - \lambda_i - \lambda_j)^\ell |\langle i | A | j \rangle|^2 \\ &= 2 \text{Tr} \left(\sum_{\ell=0}^{\infty} (\rho \otimes \mathbb{1} - \mathbb{1} \otimes \rho)^2 (\mathbb{1} \otimes \mathbb{1} - \rho \otimes \mathbb{1} - \mathbb{1} \otimes \rho)^\ell \mathbb{S}(A \otimes A) \right) \\ &\geq 2 \sum_{i,j} \sum_{\ell=0}^n (\lambda_i - \lambda_j)^2 (1 - \lambda_i - \lambda_j)^\ell |\langle i | A | j \rangle|^2 \\ &= 2 \text{Tr} \left(\sum_{\ell=0}^n (\rho \otimes \mathbb{1} - \mathbb{1} \otimes \rho)^2 (\mathbb{1} \otimes \mathbb{1} - \rho \otimes \mathbb{1} - \mathbb{1} \otimes \rho)^\ell \mathbb{S}(A \otimes A) \right) \\ &= F_n. \end{aligned} \quad (12)$$

It is clear from Eq. (12) that for any observable A and any state ρ , F_n monotonically increases ($F_{n+1} \geq F_n$), that $\forall n \in \mathbb{N}$, $F_Q \geq F_n$ and that F_n converges to F_Q as $n \rightarrow \infty$. It is also easy to check that all F_n 's are directly equal to F_Q for pure and fully mixed states (in the latter case, $F_n = F_Q = 0$).

By further expanding the powers $(\mathbb{1} \otimes \mathbb{1} - \rho \otimes \mathbb{1} - \mathbb{1} \otimes \rho)^\ell = \sum_{q=0}^{\ell} \binom{\ell}{q} (-1)^q (\rho \otimes \mathbb{1} + \mathbb{1} \otimes \rho)^q$ in Eq. (12), swapping the sums and using the *hockey-stick identity* $\sum_{\ell=q}^n \binom{\ell}{q} = \binom{n+1}{q+1}$, one can express F_n as

$$F_n = \sum_{q=0}^n \binom{n+1}{q+1} (-1)^q P_{q+2} \quad (13)$$

where

$$P_{q+2} = 2 \text{Tr} \left((\rho \otimes \mathbb{1} - \mathbb{1} \otimes \rho)^2 (\rho \otimes \mathbb{1} + \mathbb{1} \otimes \rho)^q \mathbb{S}(A \otimes A) \right) \quad (14)$$

contains the terms with an order $q+2$ in the density matrix ρ . Notice that one can also iteratively calculate each bound F_n from the previous ones and just the highest-order polynomial P_{n+2} , by writing

$$F_n = (-1)^n \left[P_{n+2} - \sum_{r=0}^{n-1} \binom{n+1}{r+1} (-1)^r F_r \right] \quad (15)$$

(which can be proven by using Eq. (13) to expand the F_r 's above, swapping the sums and using $\sum_{r=q}^{n-1} \binom{n+1}{r+1} \binom{r+1}{q+1} (-1)^r = \binom{n+1}{q+1} (-1)^{n+1}$).

Appendix B: Convergence study of our lower bounds F_n

In this section, we develop more on the convergence of our bounds F_n to F_Q for states that are neither pure, nor fully mixed. We start with

$$\frac{1}{\lambda_i + \lambda_j} - \sum_{\ell=0}^n (1 - \lambda_i - \lambda_j)^\ell = \frac{(1 - \lambda_i - \lambda_j)^{n+1}}{\lambda_i + \lambda_j}. \quad (16)$$

For any operator A , the finite distance ξ_n between F_Q and F_n can then be written as

$$\xi_n = F_Q - F_n = 2 \sum_{i,j: \lambda_i + \lambda_j > 0} \frac{(\lambda_i - \lambda_j)^2}{\lambda_i + \lambda_j} (1 - \lambda_i - \lambda_j)^{n+1} |\langle i | A | j \rangle|^2 = O(\zeta^n), \quad (17)$$

where O is the “big O notation” and with

$$\zeta = \max_{i,j: \lambda_i + \lambda_j > 0, \lambda_i \neq \lambda_j, \langle i | A | j \rangle \neq 0} (1 - \lambda_i - \lambda_j). \quad (18)$$

From the expression above, as $n \rightarrow \infty$ we thus have an exponential convergence of our bounds F_n to F_Q for any observable A and any state ρ .

To illustrate this point, let us consider a d -dimensional pure state $|\psi\rangle$, and define the corresponding state $\rho(p) = (1-p)|\psi\rangle\langle\psi| + p\mathbb{1}/d$, mixed with the fully mixed state $\mathbb{1}/d$ of noise strength p . Comparing Eqs. (10) and (17), and noting that all terms $(1 - \lambda_i - \lambda_j)$ appearing in the sum of Eq. (17) are equal to $p + 2p/d$ for such a state, we can express the finite distance ξ_n for $\rho(p)$ as

$$\xi_n = F_Q (1 - 2/d)^{n+1} p^{n+1} = (F_Q - F_0) (1 - 2/d)^n p^n \quad (19)$$

(while the explicit calculation of F_Q gives $F_Q = 4(\langle\psi|A^2|\psi\rangle - \langle\psi|A|\psi\rangle^2) \frac{(1-p)^2}{1-p+2p/d}$). The above expression enables us to see the exponential convergence ($F_Q - F_n \propto (1 - 2/d)^n p^n$) of the lower bound series F_n to F_Q for any fixed d -dimensional state $\rho(p)$ of noise strength p . In particular, we highlight this convergence feature of our bounds in Fig. 4 by considering noisy GHZ states ($|\psi\rangle = |\text{GHZ}_N\rangle$) with different values of the noise strength p , and with respect to the collective spin observable $A = \frac{1}{2} \sum_{l=1}^N \sigma_z^{(l)}$.

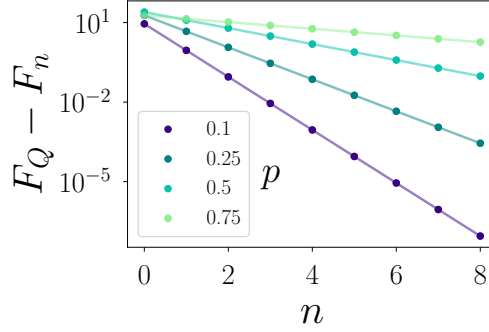


FIG. 4. *Exponential convergence of the lower bounds F_n to F_Q* — The above figure shows, for a noisy 10-qubit GHZ state and $A = \frac{1}{2} \sum_{l=1}^N \sigma_z^{(l)}$, the exponential convergence $F_Q - F_n \propto (1 - 2^{-9})^n p^n$ for various values of p (see legend). Larger values of p show a slower exponential convergence compared to smaller values of p —as also seen in Fig. 1(a)

Appendix C: Constructing unbiased estimators of the lower bounds

In this section, we elaborate on the construction of unbiased estimators of our lower bounds (such that $\mathbb{E}[\hat{F}_n] = F_n$) from the properties of U-statistics [50]. To review the protocol introduced in the main text, we perform randomized measurements on a prepared N -qubit state by applying local random unitaries $u = u_1 \otimes \dots \otimes u_n$ sampled from the CUE or a unitary 2-design followed by fixed computational basis measurements. For each distinct applied such N -qubit unitary $u^{(r)}$ followed by a measurement giving the bit-string outcome $s^{(r)}$ with $r = 1, \dots, M$, we define a single snapshot of the state *classical shadow* [44] as given previously in Eq. (5) as

$$\hat{\rho}^{(r)} = \bigotimes_{i=1}^N \left[3(u_i^{(r)})^\dagger |s_i^{(r)}\rangle \langle s_i^{(r)}| u_i^{(r)} - \mathbb{1}_2 \right], \quad (20)$$

with the classical shadow giving the state in expectation, i.e $\mathbb{E}[\hat{\rho}^{(r)}] = \rho$.

To obtain estimators of F_n , we require unbiased estimators of all P_{q+2} terms in Eq. (13) with $q = 0, \dots, n$. Using U-statistics we get estimators \hat{P}_{q+2} of P_{q+2} by replacing ρ , in each of its $q+2$ factors, by $\hat{\rho}^{(r_i)}$ with $i = 1, \dots, q+2$ and $\forall i \neq j, r_i \neq r_j$, corresponding to independent realisations of the single random unitaries $u^{(r_1)}, \dots, u^{(r_{q+2})}$. Thus we can write the estimator as

$$\hat{P}_{q+2} = \frac{2}{(q+2)!} \binom{M}{q+2}^{-1} \sum_{r_1 \neq \dots \neq r_{q+2}} \text{Tr} \left((\hat{\rho}^{(r_{q+2})} \otimes \mathbb{1} - \mathbb{1} \otimes \hat{\rho}^{(r_{q+2})}) (\hat{\rho}^{(r_{q+1})} \otimes \mathbb{1} - \mathbb{1} \otimes \hat{\rho}^{(r_{q+1})}) \prod_{i=1}^q (\hat{\rho}^{(r_i)} \otimes \mathbb{1} + \mathbb{1} \otimes \hat{\rho}^{(r_i)}) \mathbb{S}(A \otimes A) \right). \quad (21)$$

The properties of U-statistics guarantee that \hat{P}_{q+2} is an unbiased estimator of P_{q+2} i.e $\mathbb{E}[\hat{P}_{q+2}] = P_{q+2}$. From this we obtain the final expression of the estimator, using Eq. (13), as

$$\hat{F}_n = \sum_{q=0}^n \binom{n+1}{q+1} (-1)^q \hat{P}_{q+2}. \quad (22)$$

Appendix D: Deriving error bars for the lowest bound F_0

In this section we provide an analytical bound on the variance of F_0 due to the finite number of measurements M . To complement the numerical studies on the scaling of the average statistical error \mathcal{E} done in the main text, one can calculate the probabilities of our estimations of F_0 being in a given confidence interval using the Chebyshev's inequality:

$$\Pr[|\hat{F}_0 - F_0| \geq \epsilon] \leq \frac{\text{Var}[\hat{F}_0]}{\epsilon^2} \quad (23)$$

In the rest of this section, we focus on bounding the variance term $\text{Var}[\hat{F}_0]$ following a similar procedure to that previously elaborated in [28, 44], to obtain some scaling behaviors with respect to M and a lower bound on the required number of measurements M to estimate F_0 with an accuracy ϵ and for a given confidence level δ . Here, we consider unitaries from a 3-design, which allow us to use variance bounds of estimators of classical shadows. The estimate \hat{F}_0 from a finite number of measurements M can be re-written following the expression in Eq. (6) using the swap operator \mathbb{S} as

$$\hat{F}_0 = 4(\hat{h}_1 - \hat{h}_2) = \frac{4}{2!} \binom{M}{2}^{-1} \sum_{i \neq j} \text{Tr}(\hat{\rho}^{(i)} \hat{\rho}^{(j)} A^2 - \hat{\rho}^{(i)} A \hat{\rho}^{(j)} A) \quad (24)$$

$$= \frac{4}{2!} \binom{M}{2}^{-1} \sum_{i \neq j} \text{Tr}(\mathbb{S}(A^2 \otimes \mathbb{1})(\hat{\rho}^{(i)} \otimes \hat{\rho}^{(j)}) - \mathbb{S}(A \otimes A)(\hat{\rho}^{(i)} \otimes \hat{\rho}^{(j)})) \quad (25)$$

where $\hat{h}_1 = \frac{1}{2!} \binom{M}{2}^{-1} \sum_{i \neq j} \text{Tr}(\hat{\rho}^{(i)} \hat{\rho}^{(j)} A^2)$ and $\hat{h}_2 = \frac{1}{2!} \binom{M}{2}^{-1} \sum_{i \neq j} \text{Tr}(\hat{\rho}^{(i)} A \hat{\rho}^{(j)} A)$ are estimators of $h_1 = \text{Tr}(\rho^2 A^2) = \text{Tr}(\mathbb{S}(A^2 \otimes \mathbb{1})(\rho \otimes \rho)) = \mathbb{E}[\hat{h}_1]$ and $h_2 = \text{Tr}(\rho A \rho A) = \text{Tr}(\mathbb{S}(A \otimes A)(\rho \otimes \rho)) = \mathbb{E}[\hat{h}_2]$ (and where, compared to Eq. (6), we renamed the dummy indices r_1, r_2 as i, j , for later convenience). The convergence of \hat{F}_0 obtained by randomized measurements to its true value i.e $F_0 = \mathbb{E}[\hat{F}_0]$, is governed by the variance of \hat{F}_0 . We use key identities already proved in previous works [28, 44] that bound the variance of the single snapshot for a linear function $\text{Tr}(O\hat{\rho})$ (D7 in [28]) and quadratic function $\text{Tr}(O'(\hat{\rho} \otimes \hat{\rho}'))$ with O and O' being operators acting on the single and two copies of the quantum state ρ respectively and $\hat{\rho}, \hat{\rho}'$ being distinct shadows with $\hat{\rho} \neq \hat{\rho}'$. These bounds can be written as:

$$\text{Var}[\text{Tr}(O\hat{\rho})] \leq 2^N \text{Tr}(O^2), \quad (26)$$

$$\text{Var}[\text{Tr}(O'(\hat{\rho} \otimes \hat{\rho}'))] \leq 4^N \text{Tr}(O'^2). \quad (27)$$

We can bound $\text{Var}[\hat{F}_0]$ by bounding individually $\text{Var}[\hat{h}_1]$ and $\text{Var}[\hat{h}_2]$. The variance of the first term \hat{h}_1 writes

$$\text{Var}[\hat{h}_1] = \mathbb{E}[\hat{h}_1^2] - \mathbb{E}[\hat{h}_1]^2 = \frac{1}{4} \binom{M}{2}^{-2} \sum_{i \neq j} \sum_{k \neq l} \left(\mathbb{E}[\text{Tr}(\hat{\rho}^{(i)} \hat{\rho}^{(j)} A^2) \text{Tr}(\hat{\rho}^{(k)} \hat{\rho}^{(l)} A^2)] - \text{Tr}(\rho^2 A^2)^2 \right). \quad (28)$$

The above sum can be calculated by considering 3 different types of combinations of indices i, j, k and l .

1. Taking all the indices different $i \neq j \neq l \neq k$ gives $\mathbb{E}[\text{Tr}(\hat{\rho}^{(i)} \hat{\rho}^{(j)} A^2) \text{Tr}(\hat{\rho}^{(k)} \hat{\rho}^{(l)} A^2)] = \text{Tr}(\rho^2 A^2)^2$ and doesn't contribute to the variance.
2. Taking 2 indices to be the same we have 4 different combinations each giving a total of $M(M-1)(M-2)$ terms:
 - (i) $i = k$ but $j \neq l$: we get $\mathbb{E}[\text{Tr}(\hat{\rho}^{(i)} \hat{\rho}^{(j)} A^2) \text{Tr}(\hat{\rho}^{(i)} \hat{\rho}^{(l)} A^2)] = \mathbb{E}[\text{Tr}(\hat{\rho} \rho A^2)^2]$ for some generic shadow $\hat{\rho}$, yielding the variance term $\text{Var}[\text{Tr}(\hat{\rho} \rho A^2)]$.
 - (ii) $j = l$ but $i \neq k$: we have $\mathbb{E}[\text{Tr}(\hat{\rho}^{(i)} \hat{\rho}^{(j)} A^2) \text{Tr}(\hat{\rho}^{(k)} \hat{\rho}^{(j)} A^2)] = \mathbb{E}[\text{Tr}(\rho \hat{\rho} A^2)^2]$ yielding the variance term $\text{Var}[\text{Tr}(\rho \hat{\rho} A^2)]$.
 - (iii) $i = l$ but $j \neq k$: we have $\mathbb{E}[\text{Tr}(\hat{\rho}^{(i)} \hat{\rho}^{(j)} A^2) \text{Tr}(\hat{\rho}^{(k)} \hat{\rho}^{(i)} A^2)] = \mathbb{E}[\text{Tr}(\hat{\rho} \rho A^2) \text{Tr}(\rho \hat{\rho} A^2)]$ yielding the covariance term $\text{Cov}[\text{Tr}(\hat{\rho} \rho A^2), \text{Tr}(\rho \hat{\rho} A^2)]$.
 - (iv) $j = k$ but $i \neq l$: we have $\mathbb{E}[\text{Tr}(\hat{\rho}^{(i)} \hat{\rho}^{(j)} A^2) \text{Tr}(\hat{\rho}^{(j)} \hat{\rho}^{(l)} A^2)] = \mathbb{E}[\text{Tr}(\rho \hat{\rho} A^2) \text{Tr}(\hat{\rho} \rho A^2)]$ yielding the covariance term $\text{Cov}[\text{Tr}(\rho \hat{\rho} A^2), \text{Tr}(\hat{\rho} \rho A^2)]$.
3. Considering 2 pairs of equal indices we have 2 different combinations giving $M(M-1)$ terms each:
 - (i) $i = k$ and $j = l$: we have $\mathbb{E}[\text{Tr}(\hat{\rho}^{(i)} \hat{\rho}^{(j)} A^2)^2] = \mathbb{E}[\text{Tr}(\hat{\rho} \hat{\rho}' A^2)^2] = \mathbb{E}[\text{Tr}(\mathbb{S}(A^2 \otimes \mathbb{1})(\hat{\rho} \otimes \hat{\rho}'))^2]$ for some independent generic shadows $\hat{\rho}$ and $\hat{\rho}'$ yielding the variance term $\text{Var}[\text{Tr}(\hat{\rho} \hat{\rho}' A^2)] = \text{Var}[\text{Tr}(\mathbb{S}(A^2 \otimes \mathbb{1})(\hat{\rho} \otimes \hat{\rho}'))]$ with the swap-operator \mathbb{S} as we used in Eq. (25).
 - (ii) $i = l$ and $j = k$: we obtain $\mathbb{E}[\text{Tr}(\hat{\rho}^{(i)} \hat{\rho}^{(j)} A^2) \text{Tr}(\hat{\rho}^{(j)} \hat{\rho}^{(i)} A^2)] = \mathbb{E}[\text{Tr}(\hat{\rho} \hat{\rho}' A^2) \text{Tr}(\hat{\rho}' \hat{\rho} A^2)] = \mathbb{E}[\text{Tr}(\mathbb{S}(A^2 \otimes \mathbb{1})(\hat{\rho} \otimes \hat{\rho}')) \text{Tr}(\mathbb{S}(A^2 \otimes \mathbb{1})(\hat{\rho}' \otimes \hat{\rho}'))]$ giving the covariance term $\text{Cov}[\text{Tr}(\mathbb{S}(A^2 \otimes \mathbb{1})(\hat{\rho} \otimes \hat{\rho}')), \text{Tr}(\mathbb{S}(A^2 \otimes \mathbb{1})(\hat{\rho}' \otimes \hat{\rho}'))]$.

We can thus write the variance of \hat{h}_1 by taking into account all the above contributions as

$$\begin{aligned} \text{Var}[\hat{h}_1] &= \frac{M(M-1)}{4} \binom{M}{2}^{-2} \left((M-2) \left(\text{Var}[\text{Tr}(\hat{\rho}\rho A^2)] + \text{Var}[\text{Tr}(\rho\hat{\rho}A^2)] + 2\text{Cov}[\text{Tr}(\hat{\rho}\rho A^2), \text{Tr}(\rho\hat{\rho}A^2)] \right) \right. \\ &\quad \left. + \text{Var}[\text{Tr}(\mathbb{S}(A^2 \otimes \mathbb{1})(\hat{\rho} \otimes \hat{\rho}'))] + \text{Cov}[\text{Tr}(\mathbb{S}(A^2 \otimes \mathbb{1})(\hat{\rho} \otimes \hat{\rho}')), \text{Tr}(\mathbb{S}(A^2 \otimes \mathbb{1})(\hat{\rho}' \otimes \hat{\rho}))] \right). \end{aligned} \quad (29)$$

We bound the above variance by using identities in Eqs. (26)–(27) and the Cauchy-Schwartz inequality for a pair of random variables X, Y : $|\text{Cov}(X, Y)| \leq \sqrt{\text{Var}(X)\text{Var}(Y)}$ as

$$\begin{aligned} \text{Var}[\hat{h}_1] &\leq \frac{1}{M(M-1)} \left(4 \times (M-2) 2^N \text{Tr}((\rho A^2)^2) + 2 \times 4^N \text{Tr}((\mathbb{S}(A^2 \otimes \mathbb{1}))^2) \right) \\ &\leq 4 \frac{2^N \text{Tr}((\rho A^2)^2)}{M-1} + 2 \frac{4^N (\text{Tr}(A^2))^2}{(M-1)^2}. \end{aligned} \quad (30)$$

Using the cyclic permutation invariance $\text{Tr}(\hat{\rho}A\rho A) = \text{Tr}(\rho A\hat{\rho}A)$, we calculate all the contributors to the variance of \hat{h}_2 and get more directly

$$\begin{aligned} \text{Var}[\hat{h}_2] &= \frac{M(M-1)}{4} \binom{M}{2}^{-2} \left(4(M-2) \text{Var}[\text{Tr}(\hat{\rho}A\rho A)] + 2\text{Var}[\text{Tr}(\hat{\rho}A\hat{\rho}'A)] \right) \\ &= \frac{1}{M(M-1)} \left(4(M-2) \text{Var}[\text{Tr}(\hat{\rho}A\rho A)] + 2\text{Var}[\text{Tr}(\mathbb{S}(A \otimes A)(\hat{\rho} \otimes \hat{\rho}'))] \right) \\ &\leq 4 \frac{2^N \text{Tr}((A\rho A)^2)}{M-1} + 2 \frac{4^N \text{Tr}((\mathbb{S}(A \otimes A))^2)}{(M-1)^2} = 4 \frac{2^N \text{Tr}((\rho A^2)^2)}{M-1} + 2 \frac{4^N (\text{Tr}(A^2))^2}{(M-1)^2}. \end{aligned} \quad (31)$$

Comparing Eq. (30) and Eq. (31) we see that $\text{Var}[\hat{h}_1]$ and $\text{Var}[\hat{h}_2]$ could be bounded by the same quantity. The variance of \hat{F}_0 in terms of the variances of \hat{h}_1 and \hat{h}_2 can be expressed and bounded using the Cauchy-Schwartz inequality as

$$\text{Var}[\hat{F}_0] = 16\text{Var}[\hat{h}_1 + \hat{h}_2] \leq 16 \left(\sqrt{\text{Var}[\hat{h}_1]} + \sqrt{\text{Var}[\hat{h}_2]} \right)^2. \quad (32)$$

Then it follows that

$$\text{Var}[\hat{F}_0] \leq 64 \left[4 \frac{2^N \text{Tr}((\rho A^2)^2)}{M-1} + 2 \frac{4^N (\text{Tr}(A^2))^2}{(M-1)^2} \right]. \quad (33)$$

Thus, the confidence probability in Eq. (23) can be bounded as

$$\Pr[|\hat{F}_0 - F_0| \geq \epsilon] \leq \frac{\text{Var}[\hat{F}_0]}{\epsilon^2} \leq \frac{1}{\epsilon^2} \left[256 \frac{2^N \times \text{Tr}((\rho A^2)^2)}{M-1} + 128 \frac{4^N (\text{Tr}(A^2))^2}{(M-1)^2} \right]. \quad (34)$$

One can ensure that $\Pr[|\hat{F}_0 - F_0| \geq \epsilon] \leq \delta$, for a given δ , if each term of the RHS in the above equation is less than $\delta/2$. Thus it suffices to have

$$256 \frac{2^N \text{Tr}((\rho A^2)^2)}{(M-1)\epsilon^2} \leq \delta/2 \quad \text{and} \quad 128 \frac{4^N (\text{Tr}(A^2))^2}{(M-1)^2 \epsilon^2} \leq \delta/2. \quad (35)$$

Then it follows that in order to assert F_0 with a confidence level of at least $1 - \delta$ and $|\hat{F}_0 - F_0| \leq \epsilon$ for any $\delta, \epsilon > 0$, it suffices to take a number of measurements

$$M \geq \max \left\{ 512 \left(\frac{2^N \times \text{Tr}((\rho A^2)^2)}{\epsilon^2 \delta} \right) + 1, 16 \left(\frac{2^N \text{Tr}(A^2)}{\epsilon \sqrt{\delta}} \right) + 1 \right\}. \quad (36)$$

One can see from Eq. (33) that there exist two error scalings coming from the linear and quadratic terms in Eqs. (30) and (31). In the limit $M \rightarrow \infty$, the first term in Eq. (33) dominates and the standard deviation decays as $1/\sqrt{M}$ with a proportionality constant depending on the state ρ in the form of $\text{Tr}((\rho A^2)^2)$. While taking moderate or small values of M , the variance bound in Eq. (33) is dominated by the second term especially when $\text{Tr}((\rho A^2)^2)$ is small and the standard deviation decays in a faster rate proportional to $1/M$. These regimes are also captured by our numerical simulations of the error scalings. It can furthermore be noted as presented previously in [28] that the δ dependence of Eq. (36) can be improved using medians of mean estimation [44].

Appendix E: Additional numerical simulations

Here, we provide additional numerical simulations of the scalings of the statistical errors on our lower bounds F_0 and F_1 . We consider an N -qubit noisy GHZ state $\rho(p) = (1-p)|\text{GHZ}_N\rangle\langle\text{GHZ}_N| + p\mathbb{1}/2^N$ parametrized by the noise strength p . The lower bounds F_0 and F_1 are computed with respect to the observable $A = \frac{1}{2} \sum_{l=1}^N \sigma_z^{(l)}$. We simulate the protocol by applying M local random unitaries u followed by measurements in a fixed basis to obtain estimates \hat{F}_n . The average statistical error \mathcal{E} is calculated by averaging the relative error $\hat{\mathcal{E}} = |\hat{F}_n - F_n|/F_n$ with $n = 0, 1$ over 50 experimental runs for different values of M . We find the maximum value of M for which we obtain $\mathcal{E} \leq 0.1$ for different system sizes N by using a linear interpolation function. This is plotted in Fig. 5, where the scaling exponents are fitted to the obtained values of M vs N . We see that the exponential fits agree with the exponents found in the scaling analysis of the main text and remain favorable compared to quantum state tomography scalings $\sim 8^N$. The exponents a and b also highlight the fact that the measurements M needed to obtain an error \mathcal{E} is less for F_0 as compared to F_1 .

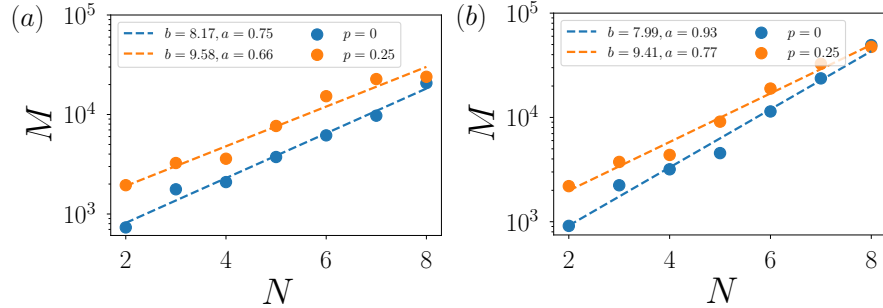


FIG. 5. *Scaling of the required number of measurements* — Panels (a) and (b) provide the number of measurements M required to estimate F_0 and F_1 respectively below an error of 0.1 for different values of p of a noisy GHZ state, with respect to $A = \frac{1}{2} \sum_{l=1}^N \sigma_z^{(l)}$. The dashed lines are exponential fits of the type 2^{b+aN} highlighting the scaling as a function of the system size N .

We now show below in Fig. 6 the non-rescaled plots of Figs. 2(b,c)-3(b,c) for GHZ and N00N states mixed with depolarization noise of strength $p = 0.25$. We estimate F_0 with a lower statistical error than F_1 for the same number of measurements M at the price of the bound F_0 being less tight compared to F_1 . Fig. 6(a,b) and Fig. 6(c,d) explicitly highlight the trade-off of the required number of measurements to estimate a tighter bound (F_1 compared to F_0) with a certain precision.

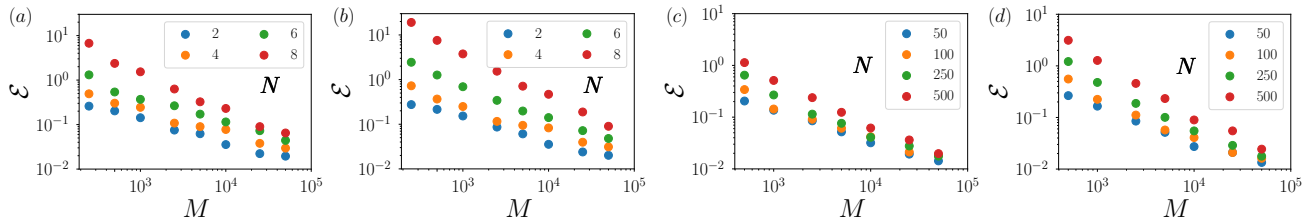


FIG. 6. *Statistical error comparisons between F_0 and F_1* — Panels (a) and (b) GHZ states and (c) and (d) N00N states, show for different system sizes N (see legends), the average statistical error for F_0 (panels (a) and (c)) and F_1 (panels (b) and (d)) as a function of the number of measurements M .